ResearchGate

See discussions, stats, and author profiles for this publication at: https://www.researchgate.net/publication/275026128

What Makes Hydroxamate a Promising Anchoring Group in Dye-Sensitized Solar Cells? Insights from Theoretical Investigation

ARTICLE *in* JOURNAL OF PHYSICAL CHEMISTRY LETTERS · JANUARY 2014

Impact Factor: 7.46

READS

23

7 AUTHORS, INCLUDING:

Ming-Li Wei

Southeast University (China)

425 PUBLICATIONS **3,335** CITATIONS

SEE PROFILE

L. G. C. Rego

Federal University of Santa Catarina

58 PUBLICATIONS **1,432** CITATIONS

SEE PROFILE

Jian Wang

Jilin University

66 PUBLICATIONS **188** CITATIONS

SEE PROFILE

Ran Jia

Technische Universität München

29 PUBLICATIONS **112** CITATIONS

SEE PROFILE

Available from: Jian Wang
Retrieved on: 30 January 2016

THE JOURNAL OF PHYSICAL CHEMISTRY Letters

Letter

pubs.acs.org/JPCL

What Makes Hydroxamate a Promising Anchoring Group in Dye-Sensitized Solar Cells? Insights from Theoretical Investigation

Wei Li,[†] Luis G. C. Rego,[‡] Fu-Quan Bai,*[,†] Jian Wang,[†] Ran Jia,[†] Li-Ming Xie,[†] and Hong-Xing Zhang*[,†]

[†]Institute of Theoretical Chemistry, State Key Laboratory of Theoretical and Computational Chemistry, Jilin University, Changchun 130023, People's Republic of China

[‡]Department of Physics, Universidade Federal de Santa Catarina, Florianopolis, Santa Catarina 88040-900, Brazil

Supporting Information

ABSTRACT: We report, from a theoretical point of view, the first comparative study between the highly water-stable hydroxamate and the widely used carboxylate, in addition to the robust phosphate anchors. Theoretical calculations reveal that hydroxamate would be better for photoabsorption. A quantum dynamics description of the interfacial electron transfer (IET), including the underlying nuclear motion effect, is presented. We find that both hydroxamate and carboxylate would have efficient IET character; for phosphate the injection time is significantly longer (several hundred femtoseconds). We also verified that the symmetry of the geometry of the anchoring group plays important roles in the electronic charge delocalization. We conclude that hydroxamate can be a promising anchoring group, as compared to carboxylate and phosphate, due to its better photoabsorption and comparable IET time scale as well as the experimental advantage of water stability. We expect the implications of these findings to be relevant for the design of more efficient anchoring groups for dye-sensitized solar cell (DSSC) application.

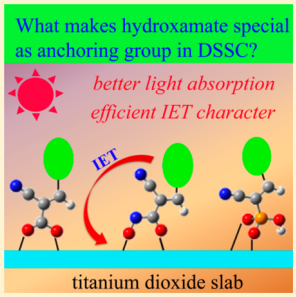

SECTION: Energy Conversion and Storage; Energy and Charge Transport

During the past two decades, with increasing concerns about environmental issues, more and more attention has been paid to the usage of renewable energy, particularly solar energy. Dye-sensitized solar cells (DSSCs) are attracting a lot of interest due to the low cost and potentially high photoelectric conversion efficiency as compared to conventional silicon-based photovoltaic devices.[1,2] In DSSCs, a dye sensitizer absorbs solar radiation and excites the electron into a wide band gap semiconductor (usually TiO_2), chosen to provide chemical stability to the device, whereas the hole created in the dye molecule is subsequently transferred to the electrolyte solution. Thus, electron−hole separation occurs at the dye/semiconductor interface. Nowadays, the highest conversion efficiency for DSSCs reaches 12.8% under AM 1.5 irradiation, which is still unsuitable for large-scale application.[3]

Ideally, the dye ought to exhibit a strong absorption band in the UV−vis spectrum, possibly reaching the near-IR region, to maximize the photon absorption efficiency. Equally important, the photoexcited electron needs to be rapidly injected to avoid the loss of the absorbed photon energy as heat through electron−phonon scattering and dissipation.[4−8] In DSSCs, the anchoring group is used to anchor dye onto the semiconductor surface, and the choice of appropriate anchoring groups is of particular importance, as they are crucial in determining the time scale of electron injection following the photoexcitation of dye. Carboxylate has become the most common anchoring group because it provides good electronic coupling on the dye−semiconductor interface, leading to efficient electron injection. Furthermore, experimentally, interfacial electron transfer (IET) with subpicosecond time scale has been reported for carboxylate anchor.[9] However, this type of anchor is vulnerable to degradation under the presence of trace quantities of water within the electrolyte, rendering it unsuitable for large-scale and long-term application.[10] The development of robust and durable as well as efficient anchors is still a fundamental concern for most theoretical and experimental groups.[10−26] Fortunately, some promising anchors for DSSC applications have been reported recently such as phosphate and hydroxamate anchors.[10,24,27] Phosphate binds strongly to TiO_2 surface, and hydroxamate is a water-stable anchor. Despite considerable interest being focused on these anchors, detailed atomistic investigations that are relevant for understanding of the underlying mechanisms responsible for the device performance, are still rare.

The main goal of this work is to address the influence of different anchoring groups—carboxylate, hydroxamate, and phosphate—on the light absorption and IET processes. Troisi and collaborators examined the dependence of IET rate on the anchoring groups by employing an approximate model that separates the system into molecular and semiconductor subsystems, while taking into account the interface between them, and subsequently computing the retarded Green's function.[25] This partition approach that, in essence, derivates from Fermi's golden rule is formulated in terms of the local density of semiconductor states at a given injection energy and the coupling between the relevant atomic orbitals. In this work

Received: September 17, 2014
Accepted: November 3, 2014
Published: November 3, 2014

 © 2014 American Chemical Society dx.doi.org/10.1021/jz501973d | J. Phys. Chem. Lett. 2014, 5, 3992−3999

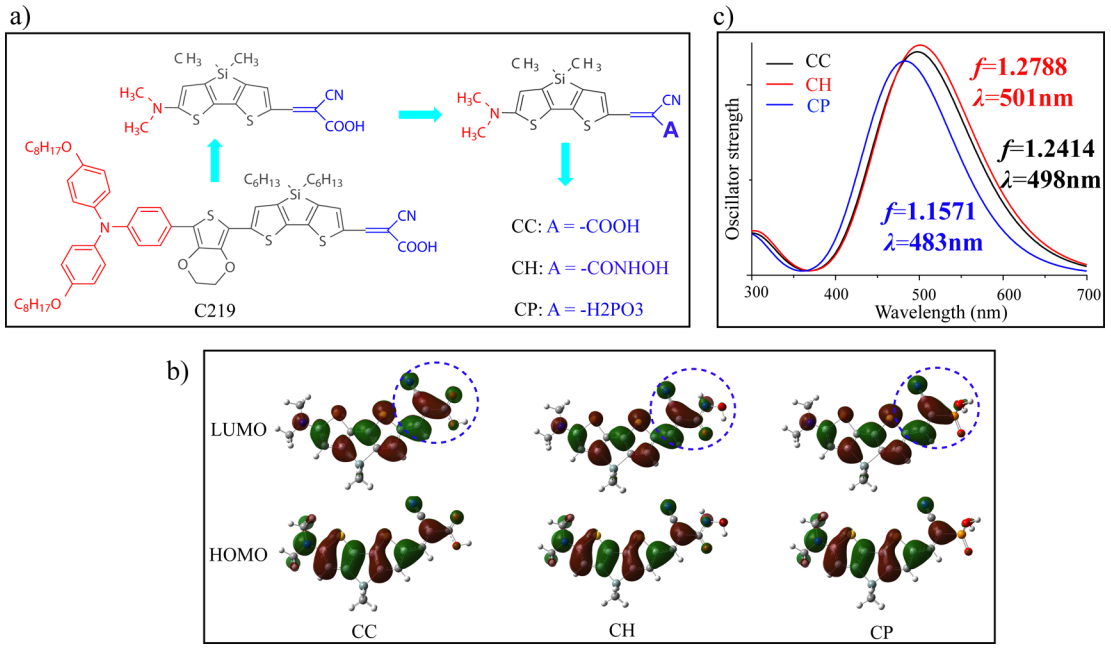

Figure 1. (a) Simplification of **C219** dye as well as the structures of dye with carboxylic anchor (**CC**), hydroxamic anchor (**CH**), and phosphoric anchor (**CP**). (b) Calculated frontier molecular orbitals. (c) Calculated absorption spectra obtained from the TD-BHandHLYP/6-31G(d) level of theory (c).

we adopt a mixed quantum-classical approach to deal with IET, where nuclear motion is treated classically, and electron dynamics is described by quantum mechanics. This mixed quantum-classical treatment has been successfully applied to investigate the photoinduced IET process in different dye–semiconductor systems.[28−31] Before describing the IET dynamics, the photoexcitation properties of free dyes will be analyzed in detail.

The metal-free **C219** dye has demonstrated viability for DSSC applications.[32] To save computational costs, we used a simplified **C219** model (Figure 1a); analogous simplification has shown that it could capture the essential character of realistic organic dyes while not changing the relative trend of the obtained results.[53] Based on this model, the dyes with carboxylate, hydroxamate, and phosphate anchors are denoted as **CC**, **CH**, and **CP**, respectively. The TiO_2 anatase (101) surface was modeled by a $(TiO_2)_{80}$ cluster comprised of two layers (5 × 4) of titanium and oxygen atoms. The geometry optimization of the free dye was performed with Guassian 09[33] at the B3LYP/6-31G(d) level of theory. For the TiO_2 cluster structure, we employed the plane-wave DFT method implemented in the Vienna ab initio simulation package (VASP), using the generalized gradient approximation (GGA) and the Perdew–Wang (PW91) exchange–correlation functional to optimize the ground state geometry of the $(TiO_2)_{80}$ cluster as well as the combined dye/TiO_2 system.[34−37] The bulk anatase TiO_2 was relaxed in a k-point mesh (5, 5, 2) with an energy cutoff of 400 eV. This set of parameters allows a force convergence within 0.01 eV/Å. We adopted the calculated lattice constants of $a = b = 3.80$ Å, and $c = 9.48$ Å, which agree well with the experimental values of 3.78 and 9.52 Å.[38] The optimized ground state structure of the dye/TiO_2 systems were used as the starting point for the adiabatic (Born–Oppenheimer) molecular dynamics (MD) simulation as carried out with the VASP package. The temperature was gradually increased from 0 to 300 K during the MD simulation, and 1.5 ps trajectories were computed with a time step of 0.5 fs.

Figure 1b shows the highest occupied molecular orbital (HOMO) and the lowest unoccupied molecular orbital (LUMO) for dyes **CC**, **CH**, and **CP**, calculated with the B3LYP/6-31G(d) level of theory. As seen from this figure, the HOMO for the three dyes is a π orbital and mainly populates the electron donor and π-bridge groups. The LUMO is a singlet π^* orbital with population more concentrated at the anchoring groups, and partially spread over the π-bridge and electron donor groups. The HOMO and LUMO orbitals of the three dyes show good overlap between the electron donor and the anchoring group, which implies fast intramolecular charge transfer.[39,40] In addition, the significant contribution of the anchoring group to LUMO provides an efficient channel for electron transport across the dye/TiO_2 interface. Notice, however, that the LUMO of **CP** has less electron residing in the anchoring moiety ($-H_2PO_3$) in comparison to the other two anchors, which reduces the coupling strength with the electronic states in the semiconductor conduction band (CB), possibly resulting in slower electron injection.

In order to examine the impact of different anchoring groups on the optical properties, time-dependent density functional theory (TDDFT) calculations on **CC**, **CH**, and **CP** were carried out. In order to obtain the optical spectrum more precisely, different functionals, such as CAM-B3LYP, BHandHLYP, PBE0, and B3LYP, were employed to calculate the absorption maxima.[39] The corresponding results are listed in Table S1. The results show no significant difference in the simulated λ_{max} for the three dyes. In addition, the relative trend of the simulated absorption maxima and oscillator strength for **CC**, **CH**, and **CP** is not altered as predicted by the four functionals. To be consistent with a previous theoretical investigation of the **C219** dye,[41] the BHandHLYP functional is chosen to simulate the absorption spectra, as shown in Figure 1c. All the absorption spectra exhibit one main absorption

dx.doi.org/10.1021/jz501973d | J. Phys. Chem. Lett. 2014, 5, 3992−3999

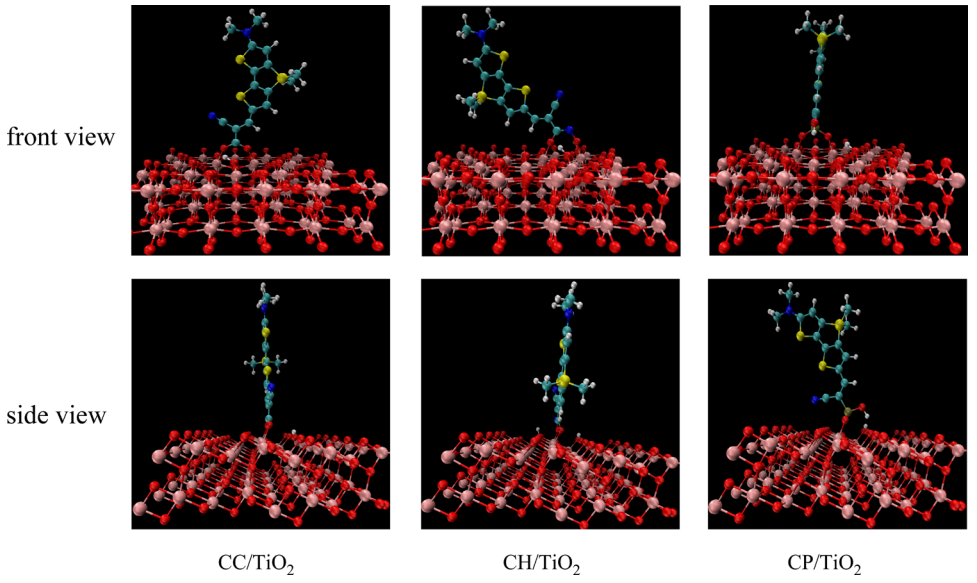

Figure 2. Optimized adsorption geometries for **CC**, **CH**, and **CP**.

band, which is not changed much by varying the anchoring group. As expected, the anchoring group does not play a significant role in the intramolecular charge transfer excitation responsible for the main transitions. Table S2 shows that the excitation from the ground state to the first excited state resulted mainly from the HOMO → LUMO transition. Nevertheless, some fine differences on the absorption are observed: (1) the λ_{max} values for **CC** and **CH** are centered at 498 and 501 nm, respectively, whereas the λ_{max} for **CP** appears at 483 nm; and (2) **CH** shows the largest oscillator strength (1.2788), as compared to **CC** (1.2414) and **CP** (1.1571). In summary, these data suggest a slightly better light-harvesting ability for the dye bearing the hydroxamate anchor, as compared to the dyes bearing carboxylate and phosphate anchors, which is in agreement with the corresponding experimental observations.[23] We believe that the impressive photoabsorption properties for dyes bearing the hydroxamate anchor can be achieved as long as the elaborate molecular modifications, i.e., on the π-spacer, are performed.[39]

In the following, we examine the adsorption of dyes on the TiO_2 anatase (101) surface. Several adsorption modes were investigated for each of the anchoring groups on this surface. For example, all three anchors can adsorb via monodentate and bidentate binding modes, directly to the TiO_2 or through a hydrogen bond.[26,42−44] Previous investigations have demonstrated that the bidentate bridging mode is one of the stable modes for these anchors on nonhydrated TiO_2 surfaces and generally leads to faster electron injection as compared to monodentate binding.[13,24−26,45] In order to make the comparison of different anchors more direct and consistent, only the bidentate bridging mode is adopted in this study, although some differences may arise for other adsorption modes.[21] Below we present details for the adsorption of these anchors; the optimized adsorption geometries are shown in Figure 2. The relevant bond lengths and adsorption energies are listed in Table 1. In the case of **CC**, the dye molecule is bound to the TiO_2 surface through bonds of its two O atoms with two surface five-coordinated Ti_{5c} atoms; the proton of the O−H group is dissociated and transferred to the surface double-coordinated O_{2c} atom near the anchoring site. The calculated adsorption energy is −1.04 eV for this case, in close

Table 1. Calculated Adsorption Energies (in eV) and Corresponding Bond Lengths (in Å)

	E_{ads}	$d(Ti-O)_1$	$d(Ti-O)_2$	$d(O_{2c}-H)$
CC	−1.04	2.02	2.05	–
CH	−0.50	1.84	1.98	–
CP	−1.52	2.01	2.01	1.69

agreement with the works by O'Rourke et al.,[21] Jiao et al.,[4] and Nilsing et al.[42] As for **CH**, its adsorption structure is completely deprotonated with the doubly bound O atom and the deprotonated O atom coordinated to two different Ti_{5c} atoms, which leads to an adsorption energy of −0.50 eV, which is smaller than that of **CC**. The two dissociated protons from the N−H and O−H groups in **CH** are bound to nearby O_{2c} atoms. It is worth noting that the obtained adsorption energy for **CH** is slightly smaller than our previous investigation (−0.67 eV).[26] Moreover, the works by Ambroiso et al.[24] and McNamara et al.[25] pointed out that hydroxamate binds to the TiO_2 surface as strongly as carboxylate, or even more strongly, which seems to contradict our results. This difference can be understood as due to the following two points:

- *The Employed Model*: In the present work, we used a large model system with the aim of examining the effect of anchoring groups on realistic dyes. The **C219** model dye, because of its long size, slanted laterally (see Figure 2), interacts with the TiO_2 surface, and produces a strain in the **CH** system. In our previous work, a small dye molecule (pyridine) was attached to the hydroxamate anchor, which maintained almost a perpendicular orientation relative to the TiO_2 surface, increasing the adsorption energy. This effect is observed for small anchoring models, as shown in the work of Ambroiso et al.
- *The Adsorption Configuration*: This work adopts the bidentate bridging mode with the doubly deprotonated configuration, which is based on the analysis from our previous theoretical study. Ambroiso et al. used the monodeprotonated form as the adsorption configuration, which exhibits slightly larger adsorption energy, but it is not dynamically stable according to MD simulations, as

dx.doi.org/10.1021/jz501973d | J. Phys. Chem. Lett. 2014, 5, 3992−3999

evinced by Figure 2 of ref 21. In the work of McNamara et al., the adsorption was described by introducing an O defect near the Ti_{5c} site, thus both O atoms of the hydroxamate chelate one surface Ti_{5c} atom. In this case, the dye is even more perpendicular to the TiO_2 surface, leading to larger adsorption energy. This work describes a defect-free TiO_2 surface.

For the **CP**/TiO_2 system, the two deprotonated oxygen atoms bind to two Ti_{5c} atoms; one of its dissociated protons is transferred to a neighboring doubly bound oxygen to form a hydroxyl group in this configuration. Furthermore, we find that the formed hydroxyl group involves hydrogen-bonding to a surface O_{2c} with a distance $d(O_{2C}-H)$ of 1.69 Å, which produces the largest adsorption energy of −1.52 eV among the three cases, in reasonable agreement with the other work.[21] Note that the position of the proton does not affect the stability very much; nevertheless, the proton prefers to bind to an under-coordinated surface O_{2c} atom, as previously suggested by Nilsing et al.[43] As discussed above, **CH** bearing hydroxamate has the smallest adsorption energy, compared with **CC** and **CP**, but the hydroxamate is more stable to water attack under highly oxidizing conditions from the experimental and applied viewpoints, which makes it preferable for DSSC application.[10,24] To obtain more information about the bonding mechanism, it is useful to investigate the charge density difference, $\Delta\rho = \rho_{dye/TiO2} - \rho_{dye} - \rho_{TiO2}$, calculated by subtracting the electronic charge of a combined dye/TiO_2 system from the individual dye and TiO_2 species, as shown in Figure S1. Plots of the charge density difference produced for adsorption by **CC**, **CH**, and **CP** systems show that notable changes occur mainly around the dye/TiO_2 interface, demonstrating the robust electronic coupling between the dye and the TiO_2 surface. For the **CP**/TiO_2 system, in particular, the charge difference plot indicates significant charge accumulation (yellow color) in the adsorbed dye, which suggests a tendency against charge transfer to TiO_2. The pronounced charge transfer occurs on the two Ti−O bonds clearly shows the formation of a strong covalent bond in the bidentate bridging configuration.

Projected density of states (DOS) calculations for the dye/TiO_2 systems were carried out with a tight-binding model Hamiltonian based on the semiempirical extended-Hückel (EH) molecular orbital theory. The method provides an excellent cost-benefit option for a clear description of energy bands, chemical bonding, and quantum dynamic processes for very large systems. The EH tight-binding Hamiltonian has been extensively applied in studies of molecular and periodic systems, including several studies of sensitized TiO_2 surfaces.[29−31,46−50] Figure S2 presents the total and projected DOS for **CC**/TiO_2, **CH**/TiO_2, and **CP**/TiO_2 systems calculated by the EH method. The calculations predict a 4.35 eV band gap for the $(TiO_2)_{80}$ model which is larger than the experimental value of 3.4 eV for the 2.4 nm particle.[51] In general, the band gap is overestimated for small TiO_2 clusters with respect to larger systems.[31] The filled red curves in Figure S2 designate the projected DOS onto electronic states of the adsorbate. This curve shows that the dye molecule introduces, upon adsorption onto TiO_2, electronic states in the semiconductor band gap region. Furthermore, the dye molecule introduces low lying unoccupied electronic states, LUMO and LUMO+1, that overlap in energy with electronic states in the TiO_2 conduction band and can give rise to the fast interfacial electron transfer. The HOMO and LUMO orbitals of the dyes gained from the EH method are shown in Figure S3. The general characteristics of the semiempirical molecular orbitals are in good agreement with the corresponding ab initio calculations.

It is, finally, important to investigate how the different anchoring groups affect the electron transfer dynamics. The quantum dynamics of the electron wavepackets is propagated by the tight-binding EH Hamiltonian according to a method described in the literature.[52] To start the IET simulation for a given dye/TiO_2 system, the electron wavepacket is initially assigned to the LUMO of dye molecule at time $t = 0$. In order to implement the nuclear dynamics, we assume that the nuclei evolves on the mean-field potential energy surface (PES), and the excited and ground electronic PESs resemble due to the similar frequencies for nuclear motion, thus nuclear trajectories can be approximated according to ab initio adiabatic molecular dynamics. The more detailed theoretical backgrounds regarding the procedure for quantum dynamics propagation of the photoexcited electron and the implementation for nuclear dynamics can be found in the Supporting Information and ref 52. $P(t)$ is the survival probability of the photoexcited electron that is still in the adsorbate molecule at time t after the photoexcitation of the system.

The simulations were carried out either in a single cell, as depicted in Figure 2, subjected to periodic boundary conditions (PBCs) in the plane of the slab, and also in 3 × 3 extended supercells constructed by repeating the single cell along the *x,y* directions, as depicted in Figure 3, also subjected to PBCs. The

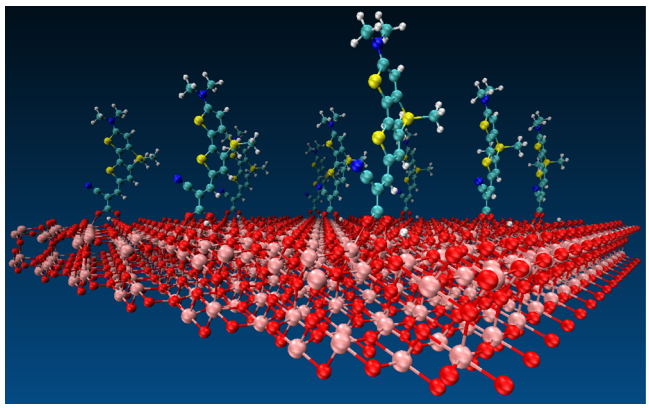

Figure 3. Dye/TiO_2 nanostructures of the constructed 3 × 3 supercells.

simulations assumed an independent electron dynamics, since the ab initio MD is independent of the wavepacket propagation. We present the results for IET simulation obtained with the 3 × 3 supercells in Figure 4a and provide the results with the single cell in the Supporting Information. The extended supercells are used to minimize the recurrences caused by the finite-size effect during the wavepacket dynamics. Nevertheless, reflections at the bottom of the TiO_2 cluster were not directly quenched, and the resulting effects can be observed in the simulations, especially as the slow decay follows the initial ultrafast electron transfer event in the **CC**/TiO_2 system. In addition, for the **CC** system, about 40% of the electronic population of dye is transferred to TiO_2 in the first 8 fs, and the slower relaxation dynamics finishes after $t \sim 200$ fs. For the **CH** system, the electron is completely injected after $t \sim 300$ fs. This injection curve can be well fitted by the exponential function:

dx.doi.org/10.1021/jz501973d | J. Phys. Chem. Lett. 2014, 5, 3992−3999

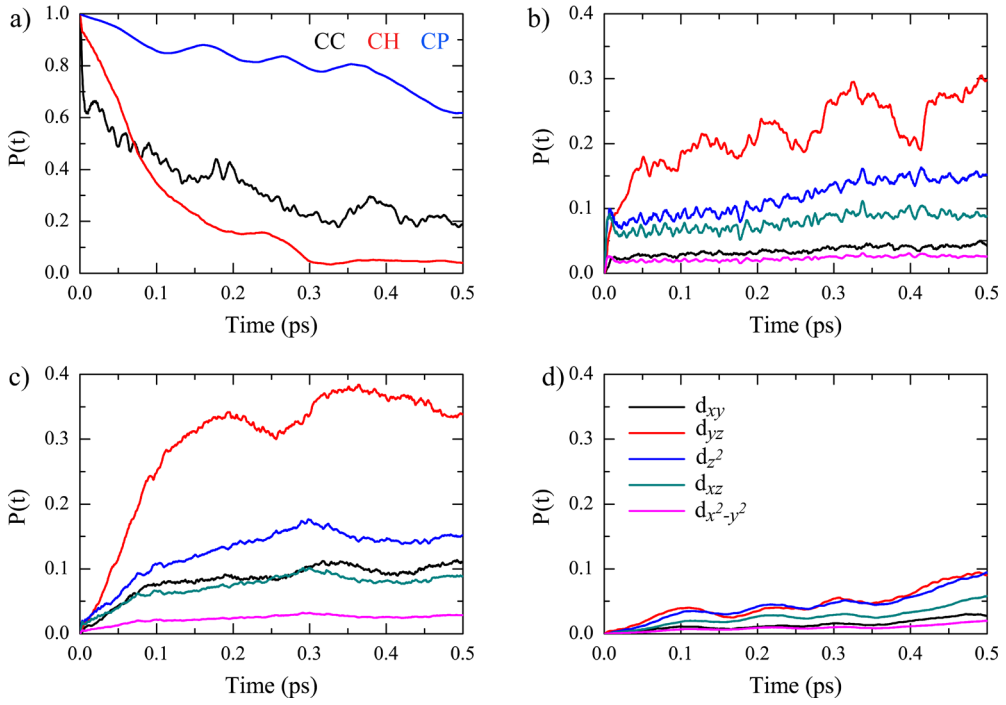

Figure 4. (a) Survival probability curves for electron injection starting from the adsorbate LUMO orbital. (b,c,d) The decomposition of the electronic population injected in the TiO_2 CB into individual populations of the Ti^{4+} d_{xy}, d_{yz}, d_{z2}, d_{xz}, and d_{x2-y2} states of **CC**/TiO_2, **CH**/TiO_2, and **CP**/TiO_2 systems, respectively.

$P(t) = 0.99 \exp(-t/0.094) + 0.034$, which allows us to conclude that the electron undergoes electron transfer from the adsorbate LUMO to the TiO_2 conduction band within a time scale of 94 fs. For the **CP** system, the IET time is significantly longer, of the order of several hundreds of femtoseconds, than the **CC** and **CH** systems. From the point of view of electron injection efficiency, the carboxylate and hydroxamate anchors are practically equivalent, and the transfer of most of the electronic charge from the adsorbate LUMO into the TiO_2 conduction band happens within the 100 fs time scale, considering the bidentate anchoring mode. The phosphate anchor, on the other hand, yields poor injection efficiency in all the simulations performed. In the work of McNamara et al., the ultrafast terahertz spectroscopy experiment revealed that the IET behavior of carboxylate-based complexes is generally identical to hydroxamate, thus rationalizing our theoretical estimations.[23]

We also carried out electron injection simulations for all the systems, keeping the nuclei fixed, to verify the role of nuclear motion and its relation to the oscillations of traces observed in Figure 4a. The corresponding results are shown in Figure S5. By comparing the traces obtained with moving versus static nuclei, we conclude the following:

- For **CC**, fast oscillations are not produced by nuclear motion. Nevertheless, after $t \sim 250$ fs, nuclear motion improves electron injection by quenching the wavepacket phase coherences that lead to recurrence originates from the reflection of electronic wavepacket at the bottom surface of the TiO_2 cluster.
- For **CH**, no significant difference is observed between the simulations carried out with or without nuclear dynamics.
- For **CP**, there is a clear indication that the oscillations observed in the electron injection traces are produced by nuclear motion. We ascribe the oscillations after the $t \sim 110$ fs period to the oscillatory motion of dye with respect to the TiO_2 surface. Although **CP** provides the largest adsorption energy (see Table 1) among the three anchors, it is also the least rigid because of the monodentate binding mode assisted by a hydrogen-bond.

Despite the equivalent efficiencies of electron injection for carboxylate and hydroxamate anchors, there are differences in the underlying electron transfer dynamics between the two cases. To disclose the origin, we also calculate the electronic time-dependent occupation on the individual Ti^{4+} orbitals (d_{xy}, d_{yz}, d_{z2}, d_{xz}, d_{x2-y2}), as shown in Figure 4b,c,d. The carboxylate and hydroxamate anchoring groups are different not only in their chemical structure but also in the geometry, that is, the symmetry of the anchoring mode, as shown in Figure 5a. In the bidentate bridging mode, the carboxylate anchor is symmetric with respect to both the (x,z) and (y,z) planes. Thus, coherent quantum dynamics through the carboxylate anchor produces a vectorial electron injection toward the bottom of the TiO_2 cluster, which is limited by the narrowness of the TiO_2 slab; the use of 3×3 extended supercells eliminates the artificial bottlenecks for delocalization in the plane of the slab (see Figures 4b and S4), and the slow decay observed for $P(t)$ is due to such surface delocalization. The d_{xy} delocalization effect is not efficient for this type of symmetric anchor, i.e., there is still a slow component in the IET simulations even using the 3×3 extended supercells. Thicker TiO_2 cluster would yield faster electron injection, that is, the initial IET event that takes place within 10−20 fs would be able to inject more electronic charge into the TiO_2 cluster. In that respect, the carboxylate anchor is analogous to the catechol anchor, except the difference in d_{xy} orbital that may be related to the H-passivated TiO_2 surface for the adsorption of catechol anchor.[30,31]

dx.doi.org/10.1021/jz501973d | J. Phys. Chem. Lett. 2014, 5, 3992−3999

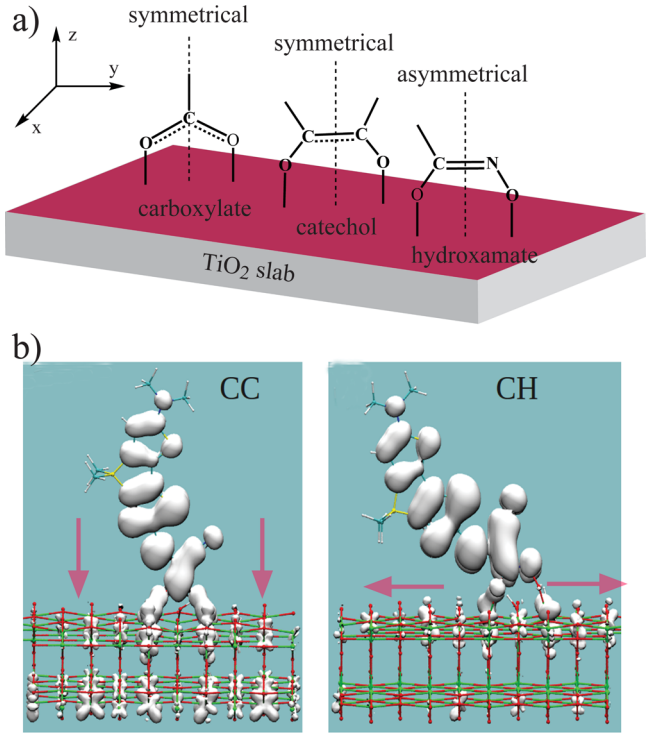

Figure 5. Illustration of the symmetry for adsorption geometry of carboxylate, catechol, and hydroxamate anchors (a) and plots of electronic isosurfaces of **CC** and **CH** systems taken at $t \sim 25$ fs (b). The red arrows indicate the direction for surface electronic charge delocalization.

As for the hydroxamate anchor, since the geometry is asymmetric, the electronic charge delocalizes much faster laterally (along the *y* direction). This effect is evinced by Figure 4c, where d_{yz} is much stronger than the other injection channels. By using 3 × 3 supercells, the IET simulations show much better injection efficiency, and the electron recurrence is almost disappeared, despite the thin TiO_2 cluster. We further show the plots of electronic isosurfaces of **CC** and **CH** systems taken at $t \sim 25$ fs in Figure 5b; this clearly suggests that, for **CH**, the electron is diffusing laterally, and is not hindered by the thickness of the slab. In comparison with the other two anchors, the phosphate anchor does not transfer much electronic charge to the Ti^{4+} d orbitals due to the weak electronic coupling with the TiO_2 conduction band; we recall that the LUMO of **CP** has less electron residing in the anchoring moiety ($-H_2PO_3$) in comparison to the other anchors. In all three systems, the d_{x2-y2} orbitals are relatively uninvolved in the IET process; this is because the bottom of the TiO_2 conduction band is mainly formed by the d_{xz}, d_{yz} and d_{xy} orbitals of the Ti^{4+}, whereas the top of the valence band is constituted principally by the d_{x2-y2} orbital. Based on the above analysis, we conclude that symmetric anchors (like the carboxylate and catechol anchors with the bidentate bridging mode) tend to guide the electronic flux perpendicularly inward from the semiconductor surface, whereas for the asymmetric anchor (such as hydroxamate anchor) the surface delocalization is concurrent to the inward injection.

In summary, this work provides a direct comparison between three anchoring groups, namely, the widely used carboxylate and the newly designed hydroxamate as well as the more robust phosphate, from a theoretical point of view. The photoexcitation properties of the free dyes, the adsorption geometries of the dye/TiO_2 systems, and the IET dynamics across the interface are discussed in detail. We conclude that hydroxamate is one promising anchoring group due to the following points: the dye with hydroxamate exhibits better light-harvesting ability because of the red-shifted absorption and larger oscillator strength. We emphasize that the good light-harvesting ability is the precondition to maximize the photocurrent response. Our computed values for the adsorption energy of the **C219** model dye on the anatase (101) surface showed that both the carboxylate and phosphate anchors produced a stronger binding than the hydroxamate anchor. Nevertheless, the water stability of hydroxamate could compensate for the smaller adsorption energy, rendering long-term durability to the device. Inspection of the IET process reveals that both carboxylate and hydroxamate anchors provided efficient IET dynamics, with a time scale of less than 100 fs. The slower injection dynamics for phosphate is due to the fact that the LUMO orbital has fewer contributions from the anchoring groups, and electronic coupling at the interface is too weak, such that substantial state mixing between the dye LUMO and TiO_2 conduction band is unlikely to occur. In addition, we also verified that the symmetry of the geometry of anchoring group influences the electronic charge delocalization: symmetric anchors guide the electronic flux perpendicularly into the semiconductor surface, whereas for the asymmetric hydroxamic anchor, the surface delocalization is concurrent to the inward injection. This work highlights, from a theoretical viewpoint, the potential of the hydroxamic anchor, which is expected to provide valuable hints into the design of a more efficient anchoring group for DSSC application.

■ ASSOCIATED CONTENT

Ⓢ Supporting Information

Additional tables and figures as well as the relevant theoretical background. This material is available free of charge via the Internet at http://pubs.acs.org.

■ AUTHOR INFORMATION

Corresponding Authors

*E-mail: baifq@jlu.edu.cn.
*E-mail: zhanghx@jlu.edu.cn.

Notes

The authors declare no competing financial interest.

■ ACKNOWLEDGMENTS

This work was supported by the Natural Science Foundation of China (Grant Nos. 21003057, 21303068, and 21173096), the State Key Development Program for Basic Research of China (Grant No. 2013CB834801), the Specialized Research Fund for the Doctoral Program of Higher Education (Grant No. 20110061110018), and the Graduate Innovation Fund of Jilin University (Grant No. 2014005). L.G.C.R. acknowledges the support by CNPq/Brazil.

■ REFERENCES

(1) O'Regan, B.; Grätzel, M. Low-Cost High-Efficiency Solar Cell Based on Dye-Sensitized Colloidal TiO_2 Films. *Nature* **1991**, *353*, 737−740.
(2) Grätzel, M. Photoelectrochemical Cells. *Nature* **2001**, *414*, 338−344.
(3) Zhang, M.; Wang, Y.; Xu, M.; Ma, W.; Li, R.; Wang, P. Design of High-Efficiency Organic Dyes for Titania Solar Cells Based on the

Chromophoric Core of Cyclopentadithiophene−Benzothiadiazole. *Energy Environ. Sci.* **2013**, *6*, 2944−2949.
(4) Jiao, Y.; Zhang, F.; Grätzel, M.; Meng, S. Structure-Property Relations in All-Organic Dye-Sensitized Solar Cells. *Adv. Funct. Mater.* **2013**, *23*, 424−429.
(5) Meng, S.; Kaxiras, E. Electron and Hole Dynamics in Dye-Sensitized Solar Cells: Influencing Factors and Systematic Trends. *Nano Lett.* **2010**, *10*, 1238−1247.
(6) Akimov, A. V.; Neukirch, A. J.; Prezhdo, O. V. Theoretical Insights into Photoinduced Charge Transfer and Catalysis at Oxide Interfaces. *Chem. Rev.* **2013**, *113*, 4496−4565.
(7) Prezhdo, O. V.; Duncan, W. R.; Prezhdo, V. V. Photoinduced Electron Dynamics at the Chromophore−Semiconductor Interface: A Time-Domain Ab Initio Perspective. *Prog. Surf. . Sci.* **2009**, *84*, 30−68.
(8) Hagfeldt, A.; Boschloo, G.; Sun, L. C.; Kloo, L.; Pettersson, H. Dye-Sensitized Solar Cells. *Chem. Rev.* **2010**, *110*, 6595−6663.
(9) Abuabara, S. G.; Rego, L. G.; Batista, V. S. Influence of Thermal Fluctuations on Interfacial Electron Transfer in Functionalized TiO_2 Semiconductors. *J. Am. Chem. Soc.* **2005**, *127*, 18234−18242.
(10) Brewster, T. P.; Konezny, S. J.; Sheehan, S. W.; Martini, L. A.; Schmuttenmaer, C. A.; Batista, V. S.; Crabtree, R. H. Hydroxamate Anchors for Improved Photoconversion in Dye-Sensitized Solar Cells. *Inorg. Chem.* **2013**, *52*, 6752−6764.
(11) Xiao, D. Q.; Martini, L. A.; Snoeberger, R. C.; Crabtree, R. H.; Batista, V. S. Inverse Design and Synthesis of acac-Coumarin Anchors for Robust TiO_2 Sensitization. *J. Am. Chem. Soc.* **2011**, *133*, 9014−9022.
(12) Martini, L. A.; Moore, G. F.; Milot, R. L.; Cai, L. Z.; Sheehan, S. W.; Schmuttenmaer, C. A.; Brudvig, G. W.; Crabtree, R. H. Modular Assembly of High-Potential Zinc Porphyrin Photosensitizers Attached to TiO_2 with a Series of Anchoring Groups. *J. Phys. Chem. C* **2013**, *117*, 14526−14533.
(13) Sodeyama, K.; Sumita, M.; O'Rourke, C.; Terranova, U.; Islam, A.; Han, L.; Bowler, D. R.; Tateyama, Y. Protonated Carboxyl Anchor for Stable Adsorption of Ru N749 Dye (Black Dye) on a TiO_2 Anatase (101) Surface. *J. Phys. Chem. Lett.* **2012**, *3*, 472−477.
(14) She, C.; Guo, J.; Irle, S.; Morokuma, K.; Mohler, D. L.; Zabri, H.; Odobel, F.; Youm, K. T.; Liu, F.; Hupp, J. T.; et al. Comparison of Interfacial Electron Transfer Through Carboxylate and Phosphonate Anchoring Groups. *J. Phys. Chem. A* **2007**, *11*, 6832−6842.
(15) Ambrosio, F.; Martsinovich, N.; Troisi, A. Effect of the Anchoring Group on Electron Injection: Theoretical Study of Phosphonated Dyes for Dye-Sensitized Solar Cells. *J. Phys. Chem. C* **2012**, *116*, 2622−2629.
(16) Katono, M.; Bessho, T.; Wielopolski, M.; Marszalek, M.; Moser, J.-E.; Humphry-Baker, R.; Zakeeruddin, S. M.; Grätzel, M. Influence of the Anchoring Modes on the Electronic and Photovoltaic Properties of D-π-A Dyes. *J. Phys. Chem. C* **2012**, *116*, 16876−16884.
(17) Wood, C.; Li, H.; Winget, P.; Brédas, J.-L. Binding Modes of Fluorinated Benzylphosphonic Acids on the Polar ZnO Surface and Impact on Work Function. *J. Phys. Chem. C* **2012**, *116*, 19125−19133.
(18) Risplendi, F.; Cicero, G.; Mallia, G.; Harrison, N. M. A Quantum-Mechanical Study of the Adsorption of Prototype Dye Molecules on Rutile-TiO_2 (110): A Comparison between Catechol and Isonicotinic Acid. *Phys. Chem. Chem. Phys.* **2013**, *15*, 235−243.
(19) Warnan, J.; Guerin, V.-M.; Anne, F. B.; Pellegrin, Y.; Blart, E.; Jacquemin, D.; Pauporté, T.; Odobel, F. Ruthenium Sensitizer Functionalized by Acetylacetone Anchoring Groups for Dye-Sensitized Solar Cells. *J. Phys. Chem. C* **2013**, *117*, 8652−8660.
(20) Koenigsmann, C.; Ripolles, T. S.; Brennan, B. J.; Negre, C. F.; Koepf, M.; Durrell, A. C.; Milot, R. L.; Torre, J. A.; Crabtree, R. H.; Batista, V. S.; et al. Substitution of a Hydroxamic Acid Anchor into the MK-2 Dye for Enhanced Photovoltaic Performance and Water Stability in a DSSC. *Phys. Chem. Chem. Phys.* **2014**, *16*, 16629−16641.
(21) O'Rourke, C.; Bowler, D. R. DSSC Anchoring Groups: A Surface Dependent Decision. *J. Phys.: Condens. Matter* **2014**, *26*, 195302−195318.
(22) Zhang, L.; Cole, J. M.; Dai, C. Variation in Optoelectronic Properties of Azo Dye-Sensitized TiO_2 Semiconductor Interfaces with Different Adsorption Anchors: Carboxylate, Sulfonate, Hydroxyl and Pyridyl Groups. *ACS Appl. Mater. Interfaces* **2014**, *6*, 7535−7546.
(23) McNamara, W. R.; Milot, R. L.; Song, H.-e.; Snoeberger, R. C., III; Batista, V. S.; Schmuttenmaer, C. A.; Brudvig, G. W.; Crabtree, R. H. Water-Stable, Hydroxamate Anchors for Functionalization of TiO_2 Surfaces with Ultrafast Interfacial Electron Transfer. *Energy Environ. Sci.* **2010**, *3*, 917−923.
(24) McNamara, W. R.; Snoeberger, R. C., III; Li, G.; Richter, C.; Allen, L. J.; Milot, R. L.; Schmuttenmaer, C. A.; Crabtree, R. H.; Brudvig, G. W.; Batista, V. S. Hydroxamate Anchors for Water-Stable Attachment to TiO_2 Nanoparticles. *Energy Environ. Sci.* **2009**, *2*, 1173−1175.
(25) Ambrosio, F.; Martsinovich, N.; Troisi, A. What Is the Best Anchoring Group for a Dye in a Dye-Sensitized Solar Cell? *J. Phys. Chem. Lett.* **2012**, *3*, 1531−1535.
(26) Li, W.; Rego, L. G. C.; Bai, F.-Q.; Kong, C.-P.; Zhang, H.-X. Theoretical Investigation of the Adsorption, IR, and Electron Injection of Hydroxamate Anchor at the TiO_2 Anatase (1 0 1) Surface. *RSC Adv.* **2014**, *4*, 19690−19693.
(27) Negre, C. F. A.; Milot, R. L.; Martini, L. A.; Ding, W.; Crabtree, R. H.; Schmuttenmaer, C. A.; Batista, V. S. Efficiency of Interfacial Electron Transfer from Zn-Porphyrin Dyes into TiO_2 Correlated to the Linker Single Molecule Conductance. *J. Phys. Chem. C* **2013**, *117*, 24462−24470.
(28) Rego, L. G. C.; Hames, B. C.; Mazon, K. T.; Joswig, J.-O. Intramolecular Polarization Induces Electron−Hole Charge Separation in Light-Harvesting Molecular Triads. *J. Phys. Chem. C* **2014**, *118*, 126−134.
(29) Hoff, D. A.; da Silva, R.; Rego, L. G. C. Coupled Electron-Hole Quantum Dynamics on D-π-A Dye-Sensitized TiO_2 Semiconductors. *J. Phys. Chem. C* **2012**, *116*, 21169−21178.
(30) Abuabara, S. G.; Rego, L. G. C.; Batista, V. S. Influence of Thermal Fluctuations on Interfacial Electron Transfer in Functionalized TiO_2 Semiconductors. *J. Am. Chem. Soc.* **2005**, *127*, 18234−18242.
(31) Rego, L. G. C.; Batista, V. S. Quantum Dynamics Simulations of Interfacial Electron Transfer in Sensitized TiO_2 Semiconductors. *J. Am. Chem. Soc.* **2003**, *125*, 7989−7997.
(32) Zeng, W. D.; Cao, Y. M.; Bai, Y.; Wang, Y. H.; Shi, Y. S.; Zhang, M.; Wang, F. F.; Pan, C. Y.; Wang, P. Efficient Dye-Sensitized Solar Cells with an Organic Photosensitizer Featuring Orderly Conjugated Ethylenedioxythiophene and Dithienosilole Blocks. *Chem. Mater.* **2010**, *22*, 1915−1925.
(33) Frisch, M. J.; Trucks, G. W.; Schlegel, H. B.; Scuseria, G. E.; Robb, M. A.; Cheeseman, J. R.; Zakrzewski, V. G.; Montgomery, J. A., Jr.; Stratmann, R. E.; Burant, J. C. et al.. *Gaussian 09*, revision A.02; Gaussian Inc.: Wallingford CT, 2009.
(34) Kresse, G.; Furthmüllerb, J. Efficiency of Ab-initio Total Energy Calculations For Metals and Semiconductors Using a Plane-Wave Basis Set. *Comput. Mater. Sci.* **1996**, *6*, 15−50.
(35) Kresse, G.; Furthmüller, J. Efficient Iterative Schemes for Ab Initio Total-Energy Calculations Using a Plane-Wave Basis Set. *Phys. Rev. B* **1996**, *54*, 11169−11186.
(36) Kresse, G.; Hafner, J. Ab Initio Molecular-Dynamics Simulation of the Liquid-Metal−Amorphous-Semiconductor Transition in Germanium. *Phys. Rev. B* **1994**, *49*, 14251−14269.
(37) Kresse, G.; Hafner, J. Ab Initio Molecular Dynamics for Liquid Metals. *Phys. Rev. B* **1993**, *47*, 558−561.
(38) Burdett, J. K.; Hughbanks, T.; Miller, G. J.; Richardson, J. W.; Smith, J. V. Structural-Electronic Relationships in Inorganic Solids: Powder Neutron Diffraction Studies of the Rutile and Anatase Polymorphs of Titanium Dioxide at 15 and 295 K. *J. Am. Chem. Soc.* **1987**, *109*, 3639−3646.
(39) Li, W.; Wang, J.; Chen, J.; Bai, F. Q.; Zhang, H. X. Theoretical Investigation and Design of High-Efficiency Dithiafulvenyl-Based Sensitizers for Dye-Sensitized Solar Cells: The Impacts of Elongating π-Spacers and Rigidifying Dithiophene. *Phys. Chem. Chem. Phys.* **2014**, *16*, 9458−9468.

(40) Li, W.; Wang, J.; Chen, J.; Bai, F. Q.; Zhang, H. X. Theoretical Investigation of Triphenylamine-Based Sensitizers with Different π-Spacers for DSSC. *Spectrochim. Acta, Part A* **2014**, *118*, 1144−1151.
(41) Zhang, J.; Li, H. B.; Geng, Y.; Wen, S. Z.; Zhong, R. L.; Wu, Y.; Fu, Q.; Su, Z. M. Modification on C219 by Coumarin Donor Toward Efficient Sensitizer for Dye Sensitized Solar Cells: A Theoretical Study. *Dyes Pigm.* **2013**, *99*, 127−135.
(42) Nilsing, M.; Persson, P.; Ojamae, L. Anchor Group Influence on Molecule−Metal Oxide Interfaces: Periodic Hybrid DFT Study of Pyridine Bound to TiO_2 via Carboxylic and Phosphonic Acid. *Chem. Phys. Lett.* **2005**, *415*, 375−380.
(43) Nilsing, M.; Lunell, S.; Persson, P.; Ojamae, L. Phosphonic Acid Adsorption at the TiO_2 Anatase (101) Surface Investigated by Periodic Hybrid HF-DFT Computations. *Surf. Sci.* **2005**, *582*, 49−60.
(44) Luschtinetz, R.; Gemming, S.; Seifert, G. Anchoring Functional Molecules on TiO_2 Surfaces: A Comparison Between the Carboxylic and the Phosphonic Acid Group. *Euro. Phys. J. Plus* **2011**, *126*, 98−110.
(45) Ambrosio, F.; Martsinovich, N.; Troisi, A. Effect of the Anchoring Group on Electron Injection: Theoretical Study of Phosphonated Dyes for Dye-Sensitized Solar Cells. *J. Phys. Chem. C* **2012**, *116*, 2622−2629.
(46) Bowman, D. N.; Blew, J. H.; Tsuchiya, T.; Jakubikova, E. Elucidating Band-Selective Sensitization in Iron(II) Polypyridine-TiO_2 Assemblies. *Inorg. Chem.* **2013**, *52*, 8621−8628.
(47) Bairu, S. G.; Mghanga, E.; Hasan, J.; Kola, S.; Rao, V. J.; Bhanuprakash, K.; Giribabu, L.; Wiederrecht, G. P.; da Silva, R.; Rego, L. G. C.; et al. Ultrafast Interfacial Charge-Transfer Dynamics in a Donor-π-Acceptor Chromophore Sensitized TiO_2 Nanocomposite. *J. Phys. Chem. C* **2013**, *117*, 4824−4835.
(48) Hoff, D. A.; Silva, R.; Rego, L. G. C. Subpicosecond Dynamics of Metal-to-Ligand Charge-Transfer Excited States in Solvated $[Ru(bpy)_3]^{2+}$ Complexes. *J. Phys. Chem. C* **2011**, *115*, 15617−15626.
(49) Rego, L. G. C.; da Silva, R.; Freire, J. A.; Snoeberger, R. C.; Batista, V. S. Visible Light Sensitization of TiO_2 Surfaces with Alq3 Complexes. *J. Phys. Chem. C* **2010**, *114*, 1317−1325.
(50) da Silva, R.; Rego, L. G. C.; Freire, J. A.; Rodriguez, J.; Laria, D.; Batista, V. S. Study of Redox Species and Oxygen Vacancy Defects at TiO_2-Electrolyte Interfaces. *J. Phys. Chem. C* **2010**, *114*, 19433−19442.
(51) Khoudiakov, M.; Parise, A. R.; Brunschwig, B. S. Interfacial Electron Transfer in Fe-II$(CN)_6^{4-}$-Sensitized TiO_2 Nanoparticles: A Study of Direct Charge Injection by Electroabsorption Spectroscopy. *J. Am. Chem. Soc.* **2003**, *125*, 4637−4642.
(52) Hoff, D. A.; Rego, L. G. *Modelling Electron Quantum Dynamics in Large Molecular Systems*; RSC Publishing: London, 2013.
(53) Ma, W.; Jiao, Y.; Meng, S. Modeling Charge Recombination in Dye-Sensitized Solar Cells Using First-Principles Electron Dynamics: Effects of Structural Modification. *Phys. Chem. Chem. Phys.* **2013**, *15*, 17187−17194.